ELSEVIER

Journal of Photochemistry and Photobiology A: Chemistry 148 (2002) 283–293

Journal of Photochemistry and Photobiology A:Chemistry

www.elsevier.com/locate/jphotochem

Enhancement of photocatalytic activity by semiconductor heterojunctions: α-Fe_2O_3, WO_3 and CdS deposited on ZnO

S. Sakthivel [a], S.-U. Geissen [b], D.W. Bahnemann [a,*], V. Murugesan [c], A. Vogelpohl [b]

[a] *Institut für Solarenergieforschung Hameln/Emmerthal (ISFH), Aussenstelle Hannover, Sokelantstr. 5, Hannover 30165, Germany*
[b] *Institute für Thermische Verfahrenstechnik, Technische Universität-Clausthal, Clausthal-Zellerfeld 38678, Germany*
[c] *Department of Chemistry, Anna University, Chennai 600025, Tamil Nadu, India*

Received 24 July 2001; received in revised form 17 October 2001; accepted 17 October 2001

Abstract

α-Fe_2O_3, WO_3 and CdS deposited on ZnO have been prepared and their photocatalytic activity was determined by photooxidation of dichloro acetic acid (DCA) in aqueous solution illuminated under medium pressure mercury lamp. These particulates were examined spectroscopically and by surface analytical methods such as surface area, X-ray diffraction (XRD) and scanning electron microscopy (SEM). The effects of the α-Fe_2O_3, WO_3 and CdS contents on the photocatalytic activities were studied. The experiments were carried out under three different conditions: (1) under continuous purging with molecular oxygen, (2) in the presence of naturally dissolved oxygen and (3) in the absence of oxygen. The results reveal that the mixtures of ZnO with α-Fe_2O_3 (0.5 wt.%), WO_3 (0.02 wt.%) and CdS (0.2 wt.%) exhibit higher photocatalytic activity than pure ZnO. © 2002 Published by Elsevier Science B.V.

Keywords: Photooxidation; Heterojunction; Zinc oxide; Iron oxide; Tungsten oxide; Cadmium sulphide; Dichloro acetic acid

1. Introduction

The photoassisted catalytic decomposition employing semiconductors as photocatalysts has been a promising method for the elimination of organic pollutants in water and in the atmosphere [1–4]. Many different photocatalysts have been used in the field of pollutants degradation. Among the various semiconductors employed, TiO_2 and ZnO are known to be good photocatalysts for the degradation of several environmental contaminants [2,5–10] due to their high photosensitivity and large bandgap, i.e. high driving force for reduction and oxidation processes, respectively. Despite the positive attributes of these photocatalysts, however, there are some drawbacks associated with their use: (i) charge carrier recombination occurs within nanoseconds [11,12] and (ii) the band edge absorption threshold does not allow the utilisation of visible light [13]. To circumvent these two particular limitations, a number of strategies have been proposed to improve the light absorption features and lengthen the carrier life time characteristics of the photocatalysts. It has been shown that the photocatalytic activity of a catalyst can be influenced by its crystal structure, surface area, size distribution, porosity, bandgap and surface hydroxyl group density [2]. Surface derivatisation of TiO_2 with a number of organic dyes extends the sensitivity of TiO_2 into the visible region [14–16] by injection of electrons from an excited level of the dye into the semiconductor conduction band. Noble metals deposited on TiO_2 have also been studied for the purpose of improving the photocatalytic activity [17–20]. Gerischer and co-workers [21–23] have proposed that the rate of photooxidation of organic compounds on the surface of a catalyst is limited by the rate of electron transfer to molecular oxygen and reported that a modification of the catalyst surface by the incorporation of noble metals can increase the efficiency of the photoassisted oxidation. Another main approach to increase the efficiency of charge separation involves the contacting of the semiconductor particle with another semiconductor. Serpone et al. [24] reported that H_2 was formed from H_2S on CdS powder illuminated with visible light in aqueous solution and that the yield was slightly increased in the presence of TiO_2 powder. The effect was explained by an improved charge separation due to electron transfer from the illuminated CdS particles into the conduction band of the TiO_2 particles. We have used a similar approach to increase the catalytic activity of ZnO by depositing another semiconductor used as a heterojunction. It is the principal goal of this work to

* Corresponding author. Present address: Universität Hannover, Institut für Technische Chemie, Callinstrasse 3, D-30167 Hannover, Germany. Tel.: +49-511-7625560; fax: +49-511-7622774.
E-mail address: bahnemann@iftc.uni-hannover.de (D.W. Bahnemann).

1010-6030/02/$ – see front matter © 2002 Published by Elsevier Science B.V.
PII: S1010-6030(02)00055-2

investigate the role of α-Fe_2O_3, WO_3 and CdS in expediting the photocatalytic oxidation reaction of ZnO. In the present study, we have prepared a number of mixed semiconductor systems in which we have introduced three different semiconductors (α-Fe_2O_3, WO_3 and CdS) to examine the effect on both the physical and the chemical characteristics, together with their influence on the photocatalytic activity of ZnO towards the photocatalytic degradation of dichloro acetic acid (DCA) used as a model pollutant. In each case the photocatalytic efficiency of α-Fe_2O_3, WO_3 and CdS loaded ZnO was compared with that of pure ZnO.

2. Experimental

2.1. Materials

Ferric nitrate, ammonium tungsten oxide, cadmium sulphide and zinc oxide were used as the starting material for the preparation of the catalysts as well as the mixed semiconductors. All chemicals were of reagent grade quality and were used as received. The water used throughout the experiment was doubly distilled.

2.2. Preparation of α-Fe_2O_3 and mixed semiconductors

α-Fe_2O_3 was obtained after 24 h hydrolysis of $Fe(NO_3)_3 \cdot 9H_2O$ at 60 °C. The colloidal solution was boiled and allowed to settle. The precipitate obtained was filtered, washed and dried in an air oven at 110 °C overnight and calcined at 420 °C for 4 h. The α-Fe_2O_3–ZnO mixed semiconductors were prepared by impregnation method. ZnO was accurately weighed and a slurry was made with the required amount of doubly distilled water. Then the desired amount of α-Fe_2O_3 was added to the ZnO slurry. The mixture was sonicated for 20 min, stirred at ambient temperature overnight and dried in an air oven at 60 °C. The dried powder was calcined at 400 °C for 4 h. Similar procedures were adopted for the preparation of WO_3–ZnO as well as CdS–ZnO. Ammonium tungsten oxide was used as a source material for WO_3.

2.3. UV–VIS diffuse reflectance spectroscopy

Absorption and reflectance spectra of pure ZnO and α-Fe_2O_3, α-Fe_2O_3, WO_3 or CdS loaded ZnO were recorded by a Bruins UV–VIS–NIR spectrophotometer equipped with an integrating sphere. $BaSO_4$ was used as a reference to measure all samples. The spectra were recorded at room temperature in air in the range 200–1400 nm enabling to study the spectral properties of these materials.

2.4. Surface area measurement

The surface area of the ZnO samples was measured by a single-point BET method using a Chemisorb 2700 (Micromeritics Instrument Co.). The samples were degassed at 170 °C for 2 h and the adsorbate gas consisted of a mixture of 30% N_2/70% He.

2.5. X-ray diffraction (XRD)

Powder XRD patterns of the ZnO samples were obtained with a Philips diffractometer with monochromated high intensity Cu Kα in the scan range 2θ between 10 and 70°.

2.6. Scanning electron microscopy (SEM)

SEM analyses were performed using a model 525 M Philips microscope.

2.7. Measurements of photocatalytic activity

The photocatalytic activity of the α-Fe_2O_3, WO_3 and CdS loaded ZnO samples was determined by monitoring the oxidation of DCA (5 mmol) in aqueous suspensions of the catalyst (1 g l^{-1}) illuminated with a 500 W medium pressure mercury lamp with a water jacket to remove IR radiation. The experiments were performed at 20 ± 1 °C, reaction mixture pH at 6.7–7.2 with three different conditions: (1) under continuous purging with molecular oxygen, (2) in the presence of naturally dissolved oxygen and (3) in the absence of oxygen. The progress of the photocatalytic degradation of DCA was followed by monitoring the change of its total organic carbon content using a TOC analyser (Shimadzu TOC-5000). The rate of TOC reduction (mg l^{-1} s^{-1}) was calculated for each run by the multiplication of the first order rate constant and the initial value of TOC content.

3. Results and discussion

3.1. UV–VIS diffuse reflectance spectroscopy

UV–VIS spectra of the bare ZnO, α-Fe_2O_3, WO_3 and CdS as well as α-Fe_2O_3, WO_3 and CdS loaded ZnO were recorded by the diffuse reflectance technique. $BaSO_4$ was used as a reference to measure all samples.

Fig. 1A illustrates the reflectance spectra of bare ZnO, α-Fe_2O_3 and 0.5 wt.% α-Fe_2O_3 loaded ZnO (optimum loading). The spectrum of bare ZnO consists of single, broad intense absorption below ca. 400 nm usually ascribed to a charge-transfer process from the valence band (mainly formed by orbitals of the oxide anions) to the conduction band (mainly formed by orbitals of the Zn^{2+} cations) [25]. Also shown are the spectral characteristics of bare α-Fe_2O_3 and α-Fe_2O_3 loaded ZnO. The reflection spectrum of α-Fe_2O_3 loaded ZnO reveals that low reflection was observed in the visible portion from 425 nm towards the visible region which is due to absorption of light by loaded α-Fe_2O_3. The light absorption characteristics of α-Fe_2O_3 loaded ZnO in the visible region are quiet similar to bulk

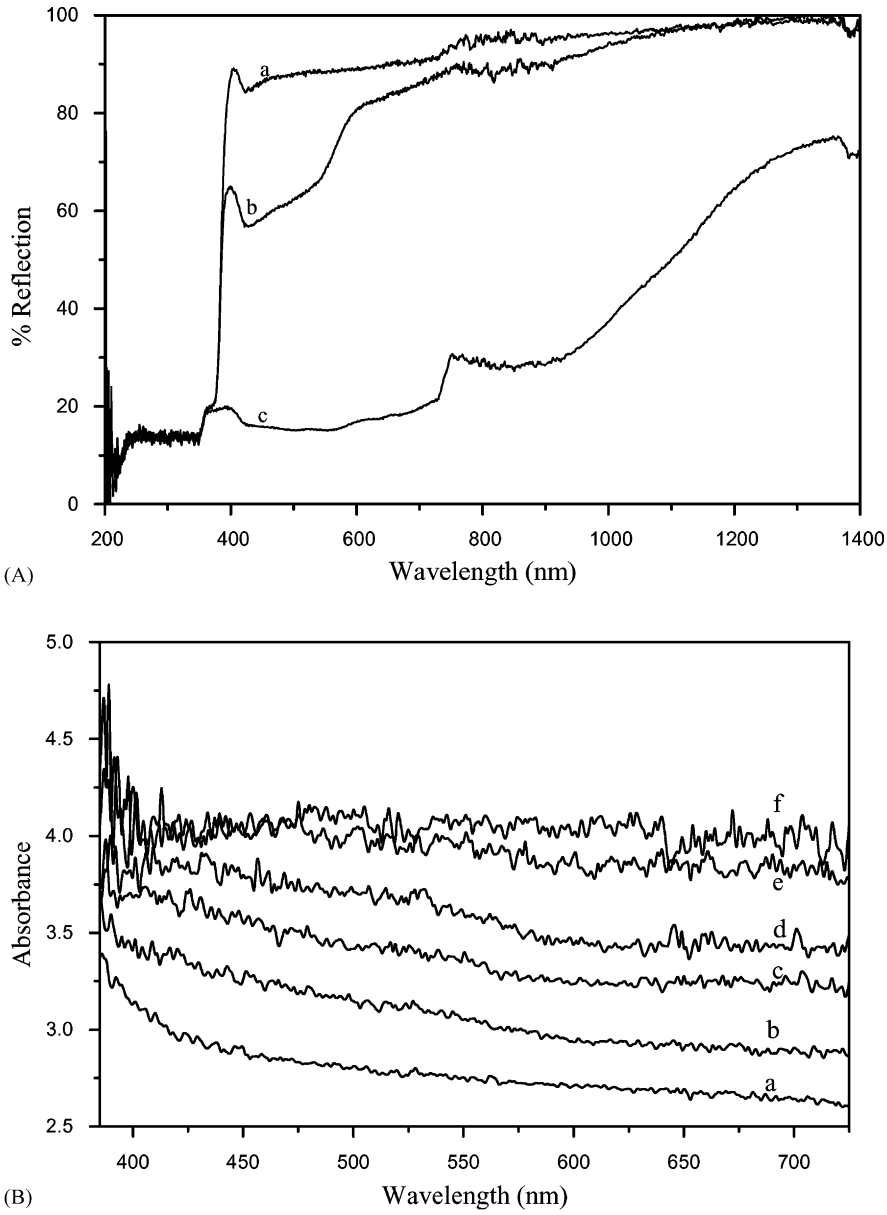

Fig. 1. (A) Reflection spectrum of bare ZnO, α-Fe_2O_3 and α-Fe_2O_3 loaded ZnO: (a) ZnO; (b) Fe–ZnO (0.5 wt.% α-Fe_2O_3); (c) α-Fe_2O_3. (B) Absorption spectra of α-Fe_2O_3 loaded ZnO samples with bare ZnO: (a) ZnO; (b) Fe–ZnO (0.05 wt.% α-Fe_2O_3); (c) Fe–ZnO (0.1 wt.% α-Fe_2O_3); (d) Fe–ZnO (0.2 wt.% α-Fe_2O_3); (e) Fe–ZnO (0.5 wt.% α-Fe_2O_3); (f) Fe–ZnO (1 wt.% α-Fe_2O_3).

α-Fe_2O_3. It is evident that α-Fe_2O_3 must have been deposited on the ZnO surface. However, it should be noted that a physical mixture of both semiconductor powders should, in principle, yield a very similar spectral response. Fig. 1B illustrates the absorption spectra of bare ZnO and α-Fe_2O_3 loaded ZnO samples. The concentration of α-Fe_2O_3 also has a marked effect on the absorption properties of ZnO. It is observed that the absorption of light in the visible region by the ZnO increased with an increase of α-Fe_2O_3 content [26].

Fig. 2A depicts the reflection spectra of WO_3 and WO_3 loaded ZnO compared with bare ZnO. WO_3 loaded ZnO samples show a reflection band similar to that recorded for the bare ZnO. Especially in the case of WO_3 loaded ZnO low reflection was observed in the whole visible range. It is obvious that WO_3 loaded on the ZnO surface absorbs a considerable amount of visible light. The results are in good agreement with previous results observed with WO_3 loaded TiO_2 [27]. Also the absorption spectrum of selected samples of WO_3 loaded ZnO and of bare ZnO are shown in Fig. 2B. The absorption band, with a maximum close to 380 nm is recorded for all WO_3–ZnO samples. The intensity of this band ascribed to a charge transfer process from oxide orbitals to W^{6+} orbitals, increases with an increase of the WO_3 loading. Similar kind of observations have been reported previously for the case of WO_3–TiO_2 [27].

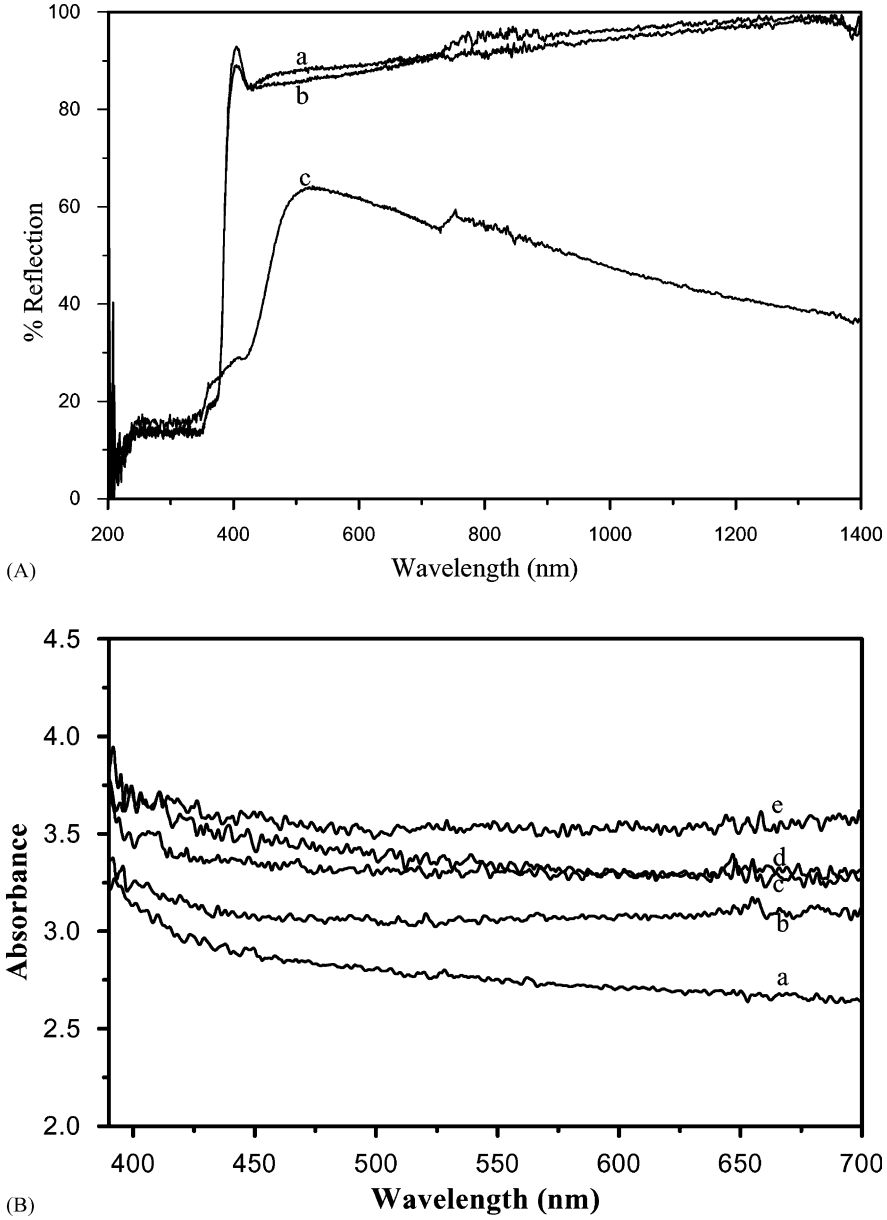

Fig. 2. (A) Reflection spectrum of bare ZnO, WO_3 and WO_3 loaded ZnO: (a) ZnO; (b) W–ZnO (0.02 wt.% WO_3); (c) WO_3. (B) Absorption spectra of WO_3 loaded ZnO samples with bare ZnO: (a) ZnO; (b) W–ZnO (0.02 wt.% WO_3); (c) W–ZnO (0.04 wt.% WO_3); (d) W–ZnO (0.06 wt.% WO_3); (e) W–ZnO (0.1 wt.% WO_3).

Fig. 3A depicts the reflection spectra of CdS and CdS loaded ZnO compared to that of bare ZnO. In the case of CdS loaded ZnO the absorption threshold extends into the visible region up to 580 nm. The absorption characteristics of CdS loaded ZnO in the visible region is similar to that of pure CdS. It is clear that CdS is apparently well dispersed on the surface of ZnO. From Fig. 3B it is noted that the absorption in the visible spectral region increases by increasing the concentration of CdS as in the case of both α-Fe_2O_3 and WO_3 loaded ZnO. As already noted in the description of Fig. 1, reflection spectra cannot differentiate between a physical mixture of two different materials or a coating of one material on top of the other. It is only by the combination of all methods employed in this study that we are convinced that dispersion of two different materials within one particle cause the observed spectra.

3.2. X-ray diffraction

XRD patterns of bare ZnO and of selected samples of α-Fe_2O_3, WO_3 and CdS loaded ZnO are shown in Fig. 4. It is observed that ZnO has hexagonal phase relative to (1 0 0), (0 0 2), (1 0 1), (1 0 2), (1 1 0), (1 0 3), (2 0 0), (1 1 2) and (2 0 1) planes, corresponding peaks are observed in

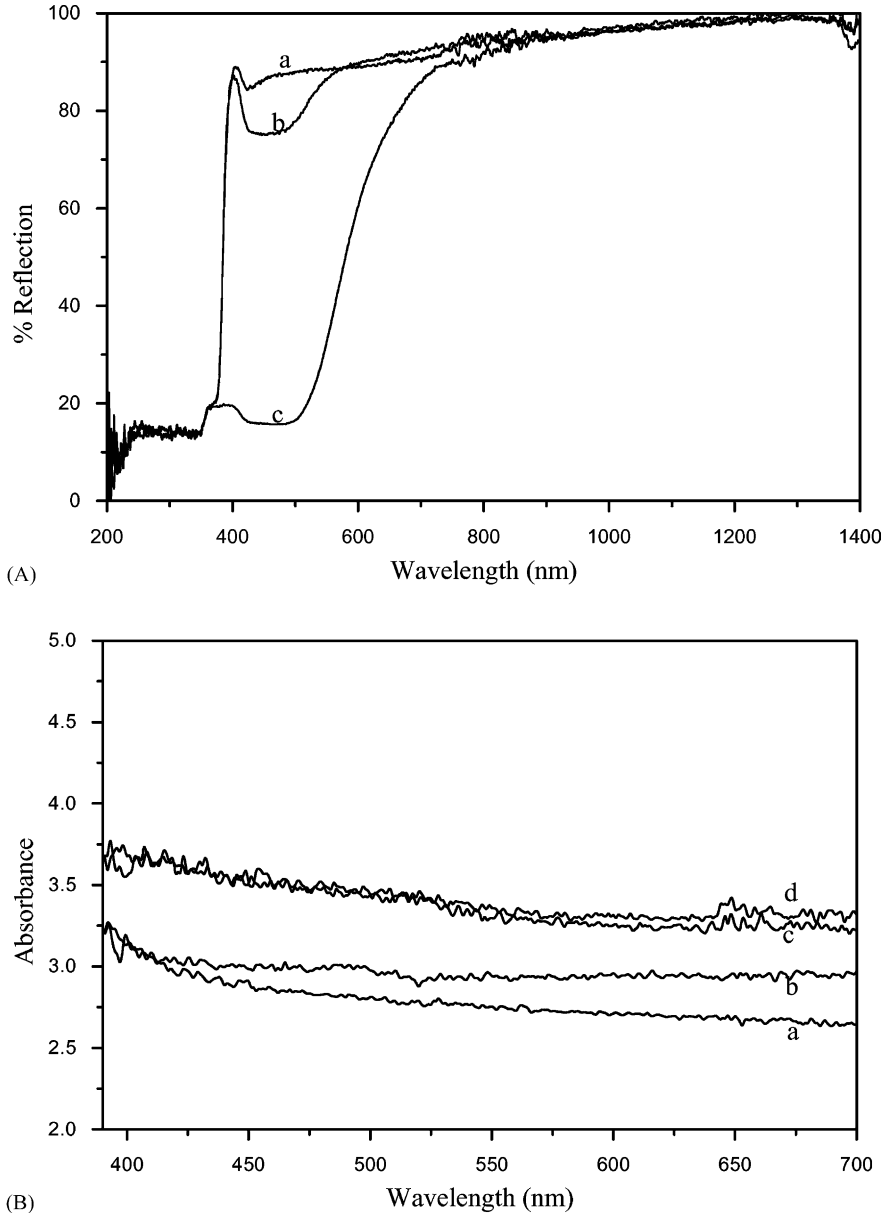

Fig. 3. (A) Reflection spectrum of bare ZnO, CdS and CdS loaded ZnO: (a) ZnO; (b) Cd–ZnO (0.2 wt.% CdS); (c) CdS. (B) Absorption spectra of CdS loaded ZnO samples with bare ZnO: (a) ZnO; (b) Cd–ZnO (0.2 wt.% CdS); (c) Cd–ZnO (0.4 wt.% CdS); (d) Cd–ZnO (0.5 wt.% CdS).

Fig. 4 starting from the left side. The XRD patterns for the α-Fe_2O_3, WO_3 and CdS loaded ZnO samples almost coincident with that of bare ZnO showing no diffraction peaks due to α-Fe_2O_3, WO_3 and CdS species, respectively, thus suggesting that these particles are either well dispersed on the ZnO surface or that the doping level is too small to detect reflections from these added semiconductors. These results are in good agreement with earlier work on mixed semiconductor particles [27].

3.3. Scanning electron microscopy

Some selected SEM micrographs of α-Fe_2O_3, WO_3 and CdS loaded ZnO samples and bare ZnO are shown in Fig. 5. No significant morphological differences among the loaded ZnO samples can be noticed by comparing the micrographs in Fig. 5. The shape of the particles for all of the samples is very similar. By comparing α-Fe_2O_3, WO_3 and CdS loaded ZnO samples with the bare ZnO it is noticed that the presence of these materials does not favour the agglomeration of the ZnO particles.

3.4. Surface area measurements

It can be seen from the surface area measurement data given in Tables 1–3 that loading of WO_3 on ZnO, WO_3 on ZnO particles does not induce any appreciable change in the surface area. However, a noticeable decrease of the surface

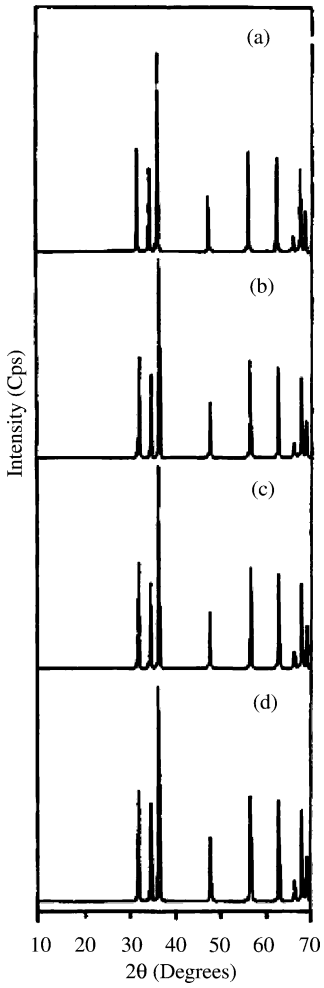

Fig. 4. XRD patterns of bare and α-Fe_2O_3, WO_3 and CdS loaded ZnO: (a) ZnO; (b) Fe–ZnO (0.5 wt.% α-Fe_2O_3); (c) W–ZnO (0.02 wt.% WO_3); (d) Cd–ZnO (0.2 wt.% CdS).

area values is observed when α-Fe_2O_3 and CdS is loaded in increasing amounts on to ZnO. While the surface area value decreases with the addition of low amounts of WO_3 (0.01 wt.%) it subsequently increases when larger amounts of WO_3 are present on the ZnO surface. This might be explained by a change of the surface properties of ZnO. Kwon et al. [28] have observed increased surface area values after the addition of WO_3 to TiO_2 and simultaneously increased Lewis surface acidity of TiO_2.

3.5. Photocatalytic activity studies

The photocatalytic oxidation of DCA was chosen as a probe reaction to study the photocatalytic activity of the α-Fe_2O_3, WO_3 and CdS loaded ZnO samples and to compare them with that of bare ZnO, α-Fe_2O_3, WO_3 and CdS. DCA has previously been used to characterise and compare the performance of different types of photocatalysts in small-scale laboratory experiments. It can conveniently be used since it has a very low vapour pressure and is soluble in water at any concentration. Also, it is a relatively strong organic acid ($pK_a = 1.29$) and therefore present in its anionic form at all pH values employed. Moreover, DCA is also an environmentally relevant pollutant, as it can be found anywhere in nature today, because it is a non-biodegradable metabolite of different chlorinated substances, such as trichloroacetic acid, perchloroethylene and others [29]. Bahnemann and co-workers [29,30,32] and Bockelmann [31] have thoroughly studied this model compound with different commercial TiO_2 and newly synthesised TiO_2 catalysts.

The photocatalytic activity results obtained by using α-Fe_2O_3, WO_3 and CdS loaded ZnO and bare ZnO, α-Fe_2O_3, WO_3 and CdS under continuous purging of molecular oxygen are reported in Tables 1–3 in the form of pseudo-first-order rate constant and initial reaction rates. The ratio between total organic carbon content at time t (TOC_t) and initial total organic carbon content (TOC_0) versus irradiation time observed during the photocatalytic degradation of DCA are shown in Figs. 6–8. The observed results from the above tables and figures indicate that the loaded α-Fe_2O_3, WO_3 and CdS samples are photocatalytically more active than the corresponding bare ZnO as well as bare α-Fe_2O_3, WO_3 and CdS. The following mechanism is proposed to explain this influence of the deposits on the photocatalytic activity. The surface deposits of α-Fe_2O_3, WO_3 or CdS on the particles of ZnO form heterojunctions resulting in a better separation of the charge carrier within the ZnO. Thus, electrons from the conduction band of the respective semiconductor particle in the mixed semiconductors

Table 1
Surface area values and photocatalytic activity results of bare ZnO, α-Fe_2O_3 and α-Fe_2O_3 loaded ZnO

Catalyst	α-Fe_2O_3 (wt.%)	BET surface area ($m^2\,g^{-1}$)	k[a] ($\times 10^5\,s^{-1}$)	R[b] ($\times 10^3\,mg\,l^{-1}\,s^{-1}$)
α-Fe_2O_3	–	33.72	0.67	0.771
ZnO	–	5.05	2.83	3.24
Fe–ZnO	0.05	4.77	9.33	10.75
Fe–ZnO	0.1	4.57	11.17	12.81
Fe–ZnO	0.2	4.50	11.22	13.07
Fe–ZnO	0.5	4.44	11.67	13.30
Fe–ZnO	1	4.37	10.33	11.84

[a] Pseudo-first-order rate constant.
[b] Initial reaction rate.

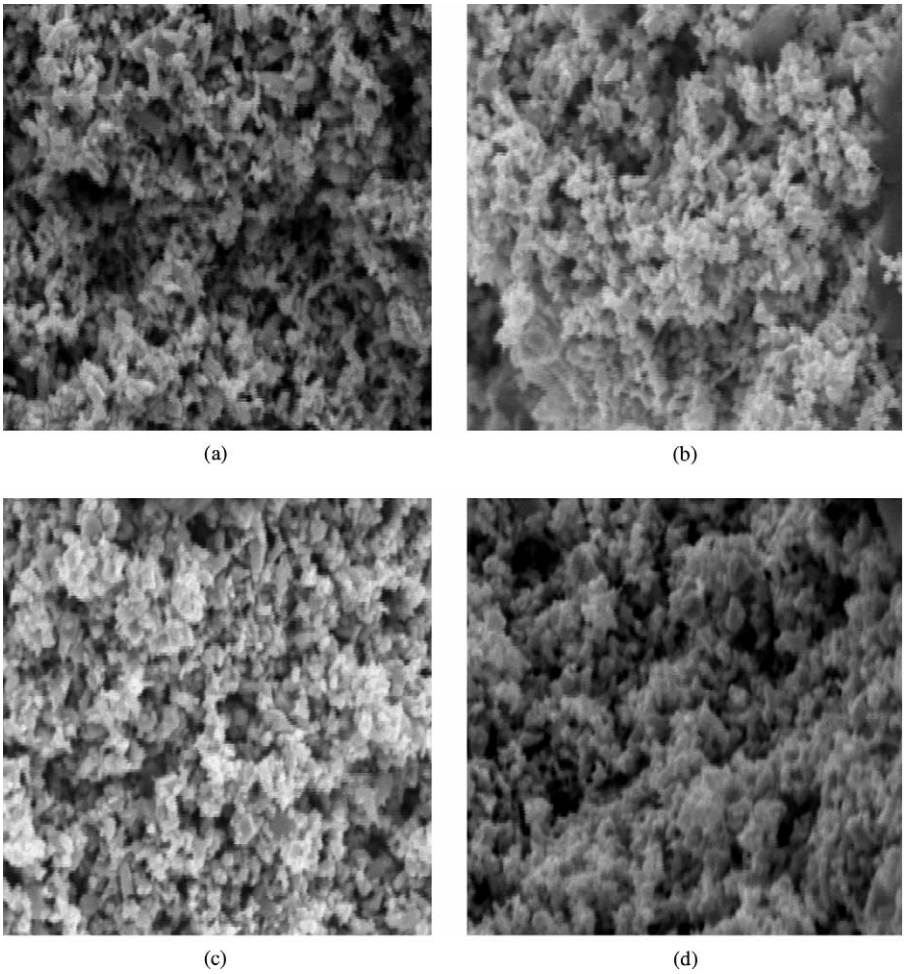

Fig. 5. SEM micrographs of bare and α-Fe_2O_3, WO_3 and CdS loaded ZnO: (a) ZnO; (b) Fe–ZnO (0.5 wt.% α-Fe_2O_3); (c) W–ZnO (0.02 wt.% WO_3); (d) Cd–ZnO (0.2 wt.% CdS).

Table 2
Surface area values and photocatalytic activity results of bare ZnO, WO_3 and WO_3 loaded ZnO

Catalyst	WO_3 (wt.%)	BET surface area ($m^2\,g^{-1}$)	k[a] ($\times 10^5\,s^{-1}$)	R[b] ($\times 10^3\,mg\,l^{-1}\,s^{-1}$)
WO_3	–	13.12	0.67	0.775
ZnO	–	5.05	2.83	3.24
W–ZnO	0.01	4.62	8.83	10.33
W–ZnO	0.02	4.64	9.33	10.81
W–ZnO	0.04	4.68	8.33	9.76
W–ZnO	0.06	4.75	8.16	9.55
W–ZnO	0.10	4.97	7.17	8.65

[a] Pseudo-first-order rate constant.
[b] Initial reaction rate.

Table 3
Surface area values and photocatalytic activity results of bare ZnO, CdS and CdS loaded ZnO

Catalyst	CdS (wt.%)	BET surface area ($m^2\,g^{-1}$)	K[a] ($\times 10^5\,s^{-1}$)	R[b] ($\times 10^3\,mg\,l^{-1}\,s^{-1}$)
CdS	–	43.88	0.50	0.58
ZnO	–	5.05	2.83	3.24
Cd–ZnO	0.1	4.84	7.00	8.09
Cd–ZnO	0.2	4.66	8.83	10.20
Cd–ZnO	0.3	4.65	6.73	7.41
Cd–ZnO	0.4	4.62	6.17	6.79
Cd–ZnO	0.5	4.60	6.00	6.61

[a] Pseudo-first-order rate constant.
[b] Initial reaction rate.

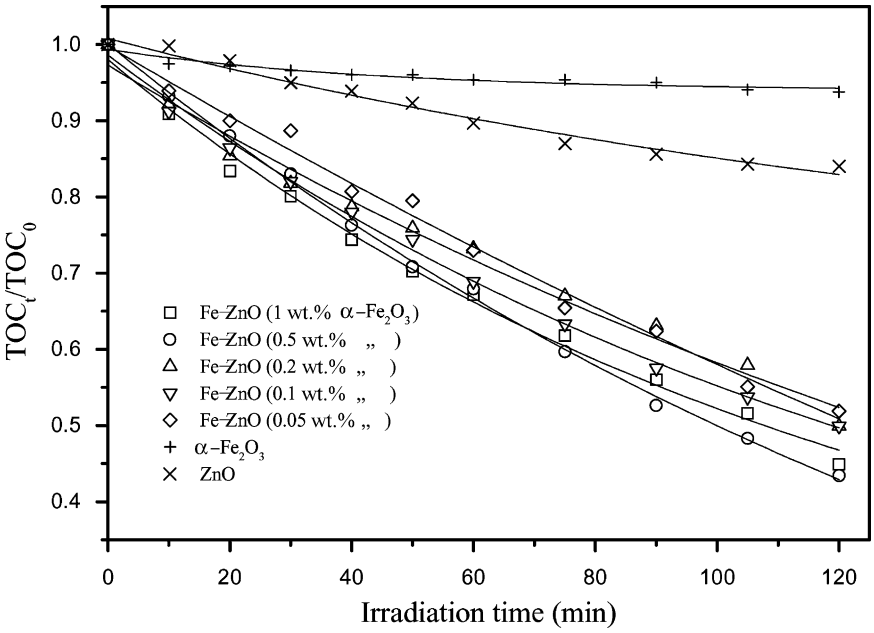

Fig. 6. Photocatalytic activity of bare ZnO, α-Fe_2O_3 and α-Fe_2O_3 loaded ZnO.

systems are transferred more easily to molecular oxygen. The remaining holes can then be transferred more efficiently to the surrounding water matrix thus accelerating the $OH^{\bullet}$ formation. Consequently, the decreased recombination rate results in an increased decomposition rate of DCA initiated by h^+ (or) $OH^{\bullet}$. Accordingly, the loading of several dispersed metals such as Pt, Au, Ag and Pd, etc. on the TiO_2 surface can expedite the transport of photoexcited electrons to suitable acceptors [33–36]. With the intend to separate the role of α-Fe_2O_3, WO_3 or CdS from that of O_2 and to distinguish between the two different effects of direct electron scavenging and subsequent reactions with radicals formed anodically experiments were carried out in the absence of oxygen. For these experiments nitrogen was continuously purged through the solutions before starting and during the experiments. The results are illustrated in Table 4. From this table it can be seen that the degradation efficiency of α-Fe_2O_3, WO_3 and CdS loaded ZnO is higher than that of bare ZnO even without oxygen being present. But the rate of degradation is much lower in nitrogen

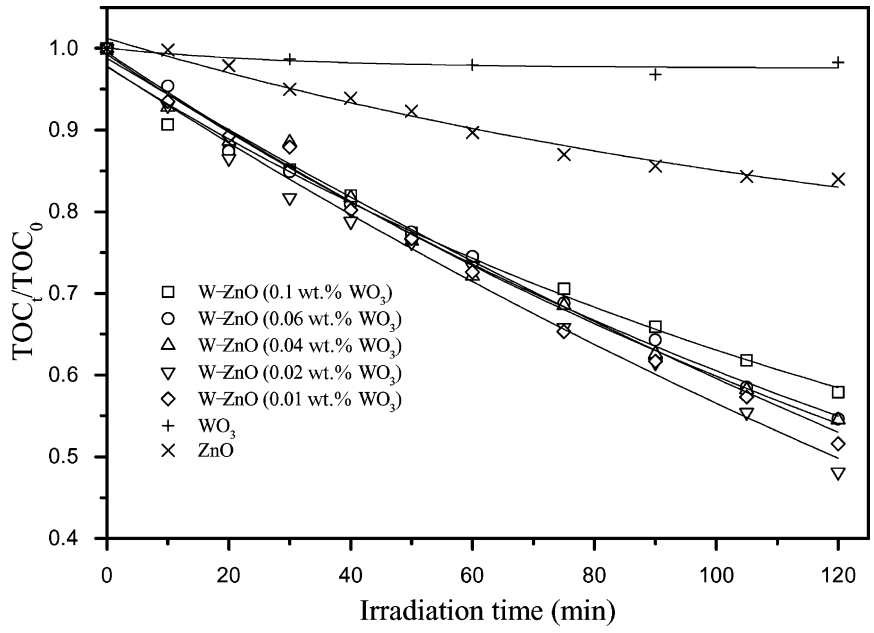

Fig. 7. Photocatalytic activity of bare ZnO, WO_3 and WO_3 loaded ZnO.

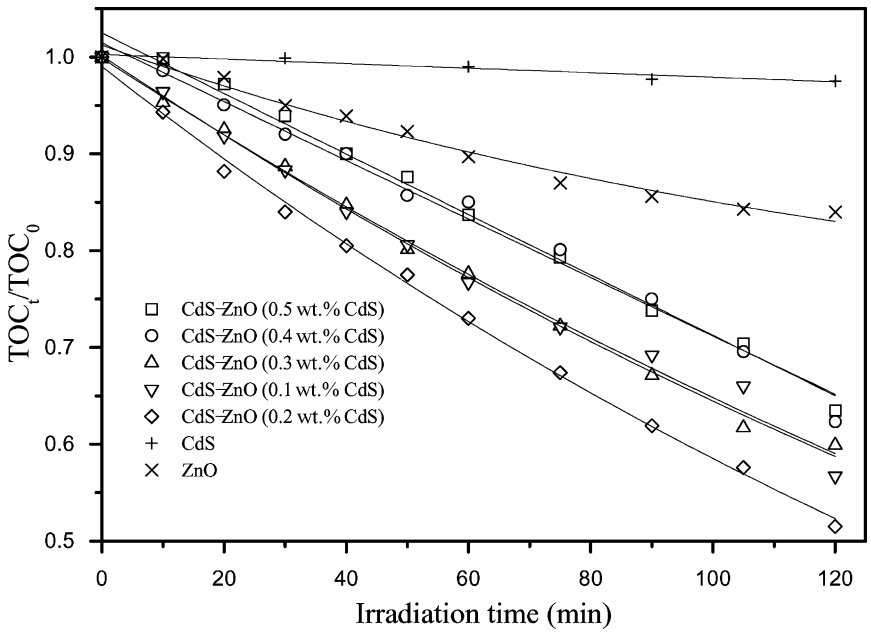

Fig. 8. Photocatalytic activity of bare ZnO, CdS and CdS loaded ZnO.

purged systems than that of experiments which were carried out with dissolved oxygen and continuous purging with molecular oxygen. The principle of charge separation in α-Fe_2O_3, WO_3 or CdS loaded ZnO systems in the presence of oxygen is illustrated in Fig. 9.

Fig. 9 illustrates the loading of α-Fe_2O_3, WO_3 or CdS on large-bandgap metal oxides such as zinc oxide (3.2 eV). Since the conduction band of ZnO is higher than that of the α-Fe_2O_3 and WO_3 except CdS, in the case of α-Fe_2O_3 and WO_3 loaded ZnO systems both α-Fe_2O_3 and WO_3 act as a sink for the photogenerated electrons. Tennakone et al. [33] and Bahnemann [26] reported that the W(VI) in WO_3 and Fe(III) in Fe_2O_3 can be easily reduced to W(V) and Fe(II), respectively. Hence, it is deduced that in the presence of WO_3 or Fe_2O_3 the electrons in the conduction band of ZnO can be easily accepted by WO_3 or Fe_2O_3, resulting in the formation of W(V) and Fe(II). These accumulated electrons in the conduction band of WO_3 or Fe_2O_3 will then be transferred to the molecular oxygen adsorbed on the surface of mixed semiconductor systems. But in contrast to the above mixed systems in CdS–ZnO system the photogenerated electrons are quickly transferred from CdS into the lower lying conduction band of a ZnO and transporting them to the molecular oxygen. Because of the much more positive potentials of the valence band in ZnO, the positive hole created by light absorption in the CdS particle remains there [34]. It has been shown in the pulse radiolysis [35] and laser flash photolysis of CdS colloids [36] that the trapped holes at the surface vacancies cause chemical changes to generate S^-_{surf}. Hotchandani and Kamat have observed the formation of S^-_{surf} by the absorption in the visible region with a maximum around 480 nm [37]. The energy difference between the two semiconductor systems prevents the reverse flow and/or recombination of the charge carriers. The rectification property of such mixed system has a beneficial effect in improving the efficiency of photooxidation. Higher sen-

Table 4
Photocatalytic activity results of bare ZnO, α-Fe_2O_3, WO_3 and CdS loaded ZnO under three reaction conditions

Catalyst	Without oxygen		Dissolved oxygen		Purging molecular oxygen	
	k[a]	R[b]	k[a]	R[b]	k[a]	R[b]
ZnO	0.33	0.41	1.00	1.14	2.83	3.24
Fe–ZnO[c]	0.51	0.61	1.33	1.58	11.67	13.30
W–Zn[d]	0.64	0.78	2.33	2.93	9.33	10.81
Cd–ZnO[e]	0.59	0.72	1.67	2.10	8.83	10.20

[a] Pseudo-first-order rate constant ($\times 10^5\ s^{-1}$).
[b] Initial reaction rate ($\times 10^3\ mg\ l^{-1}\ s^{-1}$).
[c] 0.5 wt.% α-Fe_2O_3 loaded ZnO.
[d] 0.02 wt.% WO_3 loaded ZnO.
[e] 0.2 wt.% CdS loaded ZnO.

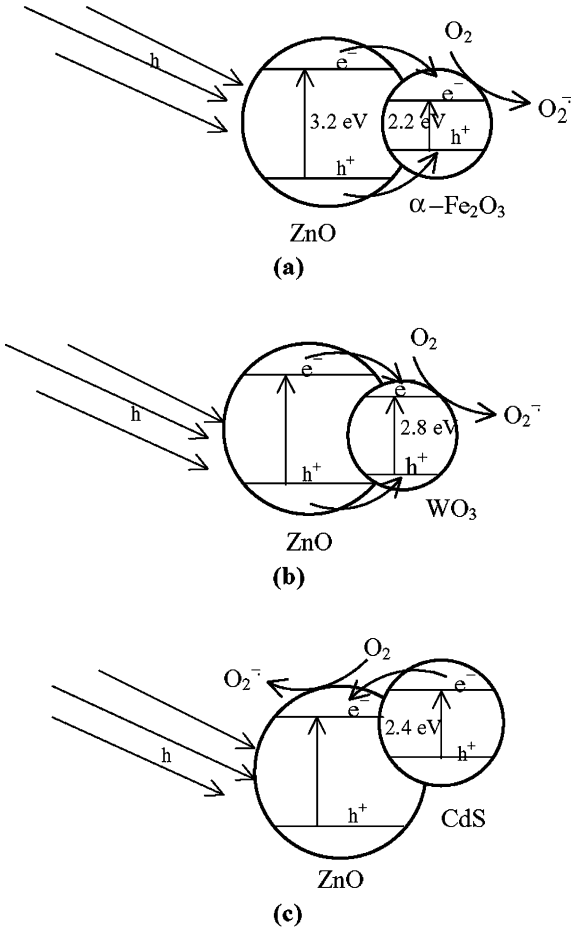

Fig. 9. The principle of charge separation in α-Fe_2O_3, WO_3 or CdS loaded ZnO systems in the presence of oxygen: (a) ZnO–α-Fe_2O_3 system; (b) ZnO–WO_3 system; (c) ZnO–CdS system.

sitisation efficiency has been reported for the sensitisation of ZnO/CdS coupled systems [38]. A five-fold enhancement in the rate of photocatalytic degradation of a DCA was observed while the experiments were carried out with continuous purging of molecular oxygen compared with experiments with actual content of dissolved oxygen in the reactant solution. Even when a little amount of a molecular oxygen is available ($7.2\,mg\,l^{-1}$) the solubility of oxygen is relatively low and oxygen is not strongly adsorbed on semiconductor surfaces in contact with aqueous electrolytes. Thus, it is hardly possible for an electron to escape recombination if it remains freely mobile in the particle. Most likely it will react with one of the still surface-adsorbed reaction products of the holes. This is the reason that we observed five-fold reduction in the rate of photocatalytic degradation of DCA while experiments were carried out with only actual content of dissolved oxygen in the reactant solution. But when the experiments were carried out with continuous purging of molecular oxygen the electrons were promptly removed by oxygen from the accumulation in one of the semiconductor particle in the mixed semiconductor system. Oxidation by holes and reduction by electrons are thus proceeding at an equal rate. The lower the steady-state concentration of electrons on the particles, the lower the recombination losses [39]. Moreover, the beneficial effect of loaded α-Fe_2O_3, WO_3 or CdS on the photocatalytic activity of ZnO is not satisfactory when experiments were carried out in the absence of oxygen, N_2 was purged before and during experiment for avoiding the role of oxygen.

Under oxygen environment the extent of charge carrier life time is considerably higher than that without oxygen. Moreover, the formation of $OH^{\bullet}$ formed through the reaction of H^+ with adsorbed water and the oxygen reduction products such as $O_2^{\bullet -}$, H_2O_2, $HO_2^{\bullet}$ which are formed through the reaction of e^- with adsorbed molecular oxygen will be enhanced in the presence of O_2. It is obvious that the degradation efficiency is comparatively higher than that in the absence of oxygen. The role of Fe_2O_3 and WO_3 has also been studied by Bahnemann and co-workers [26,41], Serpone et al. [24], Martin et al. [27], Kwon et al. [28] and Sadeghi et al. [40]. They have observed an enhancement in the rate of photoactivity by depositing these semiconductor particles on the surface of TiO_2. Furthermore we have also observed similar rate enhancement for the oxidation of DCA with increase in wt.% of Fe from 0.05 upto a maximum efficiency observed at 0.5 wt.% of Fe. At the optimum loading of 0.5 wt.% Fe the efficiency slowly decreases because spatially separating the photoelectrons from the photoholes in relatively deep Fe^{3+} traps to distances which decrease with increase in Fe^{3+} content [40]. Similar kind of negative effects have also been observed in the other mixed semiconductors systems when increasing the loading of dopant semiconductors.

4. Conclusion

α-Fe_2O_3, WO_3 and CdS semiconductors loaded on ZnO samples have been examined by spectroscopic methods as bare and as dopant semiconductors loaded ZnO. The α-Fe_2O_3, WO_3 and CdS loaded ZnO systems show an absorption threshold extended into the visible region due to the light absorption characteristics of loaded semiconductors in the visible region. α-Fe_2O_3, WO_3 and CdS loaded ZnO samples show a higher photocatalytic activity than bare ZnO when the experiments were carried out using all the three conditions such as (1) under continuous purging with molecular oxygen, (2) in the presence of naturally dissolved oxygen and (3) in the absence of oxygen. A three-fold enhancement in the rate of the photocatalytic degradation of DCA was observed when the experiments were carried out in the presence of oxygen rather than under nitrogen atmosphere. This is explained by an enhanced scavenging of the photogenerated electrons by O_2. Moreover, the photocatalytic activity was greatly influenced by continuous purging with molecular oxygen. Under these conditions the electrons are promptly removed from one of the semiconductor particles in the mixed semiconductor system. Oxidation by

holes and reduction by electrons are proceeding at an equal rate. The lower the steady-state concentration of electrons on the particles, the lower the recombination losses. Hence, it can be concluded that the main role of α-Fe_2O_3, WO_3 and CdS as heterojunctions, is the improved separation of photoproduced electron/hole pairs and, consequently, results in the observed higher photocatalytic activity.

Acknowledgements

The authors gratefully acknowledge the financial support extended by DAAD, Germany to Mr. S. Sakthivel through fellowship to carryout his research work in Germany.

References

[1] D.F. Ollis, C.S. Turchi, Environ. Prog. 9 (1990) 229.
[2] D.W. Bahnemann, in: E. Pelizzetti, M. Schiavello (Eds.), Photochemical Conversion and Storage of Solar Energy, Kluwer Academic Publishers, Dordrecht, 1991, pp. 251–276.
[3] M.R. Hoffmann, S.T. Martin, W. Choi, D.W. Bahnemann, Chem. Rev. 95 (1995) 69.
[4] A. Mills, S.L. Hunte, J. Photochem. Photobiol. A: Chem. 108 (1997) 1.
[5] K.I. Okamoto, Y. Yamamoto, H. Tanaka, M. Tanaka, Bull. Chem. Soc. Jpn. 58 (1985) 2015.
[6] V. Augugliaro, L. Palmisano, M. Schiavello, A. Sclafani, L. Marchose, G. Martra, F. Mians, Appl. Catal. 69 (1991) 323.
[7] H. Ohnishi, M. Matsumura, H. Tsubomura, M. Iwasaki, Ind. Eng. Chem. Res. 28 (1989) 719.
[8] A. Sharma, P. Rao, R.P. Mathur, S.C. Ametha, J. Photochem. Photobiol. A: Chem. 86 (1995) 197.
[9] S. Sakthivel, B. Neppolian, M. Palanichamy, B. Arabindoo, V. Murugesan, Indian J. Chem. Tech. 6 (1999) 161.
[10] S. Sakthivel, B. Neppolian, B. Arabindoo, M. Palanichamy, V. Murugesan, Water Sci. Tech. 44 (2001) 211.
[11] G. Rothenberger, J. Moser, M. Grätzel, N. Serpone, D.K. Sharma, J. Am. Chem. Soc. 107 (1985) 8054.
[12] N. Serpone, E. Pelizzetti, Photocatalysis: Fundamentals and Applications, Wiley, New York, 1989, p. 342.
[13] N. Serpone, D. Lawless, J. Disdier, J.-M. Herrmann, Langmuir 10 (1994) 643.
[14] J. Moser, M. Grätzel, J. Am. Chem. Soc. 106 (1984) 6557.
[15] R.W. Fessenden, P.V. Kamat, Chem. Phys. Lett. 123 (1984) 233.
[16] P.V. Kamat, J.P. Chauret, R.W. Fessenden, J. Phys. Chem. 90 (1986) 1389.
[17] T. Sakata, T. Kawai, K. Hashimoto, Chem. Phys. Lett. 88 (1982) 50.
[18] L.R. Faulkner, Chem. Eng. News 27 (1984) 28.
[19] J. Abrahams, R.S. Davidson, C.J. Morrison, Photochem. Photobiol. A: Chem. 29 (1985) 353.
[20] R.P.S. Suri, J. Liu, D.W. Hand, J.C. Crittenden, D.L. Perram, M.E. Mullins, Water Environ. Res. 65 (1993) 665.
[21] H. Gerischer, A. Heller, J. Phys. Chem. 95 (1991) 5261.
[22] H. Gerischer, in: D.F. Ollis, H. Al-Ekabi (Eds.), Photocatalytic Purification and Treatment of Water and Air, Elsevier, New York, 1993, p. 1.
[23] C.M. Wang, A. Heller, H. Gerischer, J. Am. Chem. Soc. 114 (1992) 5230.
[24] N. Serpone, E. Borgarello, M. Grätzel, J. Chem. Soc. Commun. (1983) 342.
[25] E. Borgarello, J. Kiwi, M. Grätzel, E. Pelizzetti, M. Visca, J. Am. Chem. Soc. 104 (1982) 2996.
[26] D.W. Bahnemann, Isr. J. Chem. 33 (1993) 115.
[27] C. Martin, G. Solana, V. Rives, G. Marci, L. Polmisano, A. Sclafani, Catal. Lett. 49 (1997) 235.
[28] Y.T. Kwon, K.Y. Song, W.I. Lee, G.J. Choi, Y.R. Do, J. Catal. 191 (2000) 192.
[29] D.W. Bahnemann, D. Bockelmann, R. Goslich, M. Hilgendorft, D. Weichgrebe, Trace metal in the environment, in: D.F. Ollis, H. Al-Ekabi (Eds.), Photocatalytic Purification and Treatment of Water and Air, Elsevier, Amsterdam, 1993, p. 301.
[30] D.W. Bahnemann, D. Bockelmann, R. Koslich, M. Hilgendorft, in: G.R. Helz, R.G. Zepp, D.G. Crosby (Eds.), Aquatic and Surface Photochemistry, Lewis, Boca Raton, 1994, p. 349.
[31] D. Bockelmann, Solare Reinigung Verschmutzter Wässer mittels Photocatalyse, Ph.D. Thesis, Technical University of Clausthal, Cuvillier, Verlag, Göttingen, 1994.
[32] M. Lindner, D.W. Bahnemann, B. Hirthe, W.-D. Greibler, ASME J. Sol. Energy Eng. 119 (1997) 399.
[33] K. Tennakone, O.A. Heperuma, J.M.S. Bandara, W.C.B. Kiridena, Semicond. Sci. Technol. 7 (1992) 423.
[34] L. Spanhel, H. Weller, A. Henglein, J. Am. Chem. Soc. 109 (1987) 6632.
[35] S. Baral, A. Fojtik, H. Weller, A. Henglein, J. Am. Chem. Soc. 108 (1986) 375.
[36] P.V. Kamat, T.W. Ebhesen, N.M. Dimitrijevic, A.J. Nozik, Chem. Phys. Lett. 157 (1989) 384.
[37] S. Hotchandani, P.V. Kamat, J. Phys. Chem. 96 (1992) 6834.
[38] S. Hotchandani, P.V. Kamat, Chem. Phys. Lett. 191 (1992) 320.
[39] H. Gerischer, A. Heller, J. Phys. Chem. 95 (1991) 5261.
[40] M. Sadeghi, W. Liu, T.G. Zhong, P. Stavropoulos, B.J. Levy, J. Phys. Chem. 100 (1996) 19466.
[41] D. Bockelmann, M. Lindner, D.W. Bahnemann, in: E. Pellizzetti (Ed.), Fine Particle Science and Technology from Micro to Nanoparticles, NATO ASI Series 3, High Technology, Vol. 12, Kluwer Academic Publishers, Dordrecht, 1996, pp. 675–689.